

"Intact nephrons" as the primary origin of proteinuria in chronic renal disease. Study in the rat model of subtotal nephrectomy.

T Yoshioka, ... , J R Hoyer, I Ichikawa

J Clin Invest. 1988;**82**(5):1614-1623. <https://doi.org/10.1172/JCI113773>.

Research Article

Single nephron filtration rate of albumin (SNGFRAIb) was measured in remnant nephrons of Munich-Wistar rats 4-6 wk after subtotal nephrectomy (NPX). Serial thin-section histological analysis was then conducted on the same glomeruli by light microscopy. SNGFRAIb ranged from 1 to 15 times normal. However, a direct relationship between abnormalities of structure and function was not seen, e.g. the glomeruli with the fewest structural abnormalities and marked hyperfiltration often had the highest SNGFRAIb. Moreover, the majority of glomeruli had minimal structural abnormalities. Normalization of the markedly elevated glomerular capillary pressure (PGC) in these glomeruli was accomplished by acute intravenous infusion of verapamil, which decreased SNGFRAIb by 9-83% without affecting the single nephron filtration rate of water (SNGFRH₂O). 1-2 wk after subtotal NPX, all glomeruli were hyperfiltering and had elevated PGC. The fractional clearance of larger (greater than 36 Å) dextrans was selectively increased in these glomeruli that lacked discernible damage by light microscopy. Verapamil normalized PGC, reduced proteinuria to 48 ± 4% of baseline, and improved glomerular size selectivity without altering SNGFRH₂O. Proteinuria after subtotal NPX thus originates largely from glomeruli with minimal structural abnormalities. The defect in size selectivity is largely attributed to the prevailing high PGC, producing large, nonselective channels on the glomerular capillary wall. The observations raise the possibility that in chronic renal diseases, the reduction in proteinuria [...]

Find the latest version:

<https://jci.me/113773/pdf>



"Intact Nephrons" as the Primary Origin of Proteinuria in Chronic Renal Disease

Study in the Rat Model of Subtotal Nephrectomy

Toshimasa Yoshioka,* Hiroshi Shiraga,† Yoshiyuki Yoshida,* Agnes Fogo,‡ Alan D. Glick,§ William M. Deen,||

John R. Hoyer,‡ and Iekuni Ichikawa*

*Department of Pediatrics, Vanderbilt University School of Medicine, Nashville, Tennessee 37232; †Department of Pediatrics, University of Pennsylvania School of Medicine, Philadelphia, Pennsylvania 19104; ‡Department of Pathology, Vanderbilt University School of Medicine, Nashville, Tennessee 37232; and ||Department of Chemical Engineering, Massachusetts Institute of Technology, Cambridge, Massachusetts 02139

Abstract

Single nephron filtration rate of albumin (SNGFR_{Alb}) was measured in remnant nephrons of Munich-Wistar rats 4–6 wk after subtotal nephrectomy (NPX). Serial thin-section histological analysis was then conducted on the same glomeruli by light microscopy. SNGFR_{Alb} ranged from 1 to 15 times normal. However, a direct relationship between abnormalities of structure and function was not seen, e.g. the glomeruli with the fewest structural abnormalities and marked hyperfiltration often had the highest SNGFR_{Alb}. Moreover, the majority of glomeruli had minimal structural abnormalities. Normalization of the markedly elevated glomerular capillary pressure (P_{GC}) in these glomeruli was accomplished by acute intravenous infusion of verapamil, which decreased SNGFR_{Alb} by 9–83% without affecting the single nephron filtration rate of water (SNGFR_{H₂O}). 1–2 wk after subtotal NPX, all glomeruli were hyperfiltering and had elevated P_{GC}. The fractional clearance of larger (> 36 Å) dextrans was selectively increased in these glomeruli that lacked discernible damage by light microscopy. Verapamil normalized P_{GC}, reduced proteinuria to 48±4% of baseline, and improved glomerular size selectivity without altering SNGFR_{H₂O}. Proteinuria after subtotal NPX thus originates largely from glomeruli with minimal structural abnormalities. The defect in size selectivity is largely attributed to the prevailing high P_{GC}, producing large, nonselective channels on the glomerular capillary wall. The observations raise the possibility that in chronic renal diseases, the reduction in proteinuria often seen after therapeutic measures, including antihypertensive medication, may reflect their functional effect on the relatively intact glomeruli rather than their structure-sparing effect on severely damaged glomeruli, which contribute little to the proteinuria.

Introduction

Chronic renal diseases resulting from a variety of causes share several common functional features, one of which is protein-

Portions of these studies were presented at the Annual Meeting of the American Society of Nephrology, Washington, DC, December 1986, and were published in abstract form in *Kidney Int.* 1987. 31:424. (Abstr.)

Address reprint requests to Dr. T. Yoshioka, C-4204, M. C. N., Vanderbilt University Medical Center, Nashville, TN 37232.

Received for publication 6 July 1987 and in revised form 25 April 1988.

J. Clin. Invest.

© The American Society for Clinical Investigation, Inc.

0021-9738/88/11/1614/10 \$2.00

Volume 82, November 1988, 1614–1623

uria. The physiology underlying the nonselective nature of the proteinuria has recently been investigated by Myers and his associates (1, 2) in patients with a variety of primary glomerulopathies. An impairment of molecular size-selective function of glomeruli in these diseases has been illustrated. However, because the renal histology in chronic diseases is often characterized by a marked nephron-to-nephron heterogeneity, the nature of specific histological changes that primarily account for the proteinuria in chronic renal diseases has not been defined.

The rat model of subtotal nephrectomy (NPX) possesses several characteristics that are typically seen in human chronic renal diseases. In addition to marked structural heterogeneity, progressive azotemia, proteinuria, and glomerular sclerosis are present in this model (3–6). Note that conventional methodology such as whole-kidney clearance measurements, does not allow the structure-function relationship among nephrons in kidneys with focal lesions to be evaluated directly. In this regard, Munich-Wistar rats are uniquely endowed with glomeruli on the surface of the kidney. This location allows the collection of single glomerular filtrate and measurement of various glomerular hemodynamic parameters, and these same glomeruli are also readily identified topographically for subsequent histological examination (7, 8). In this study, therefore, the level of albumin filtration and the severity of glomerular sclerosis were assessed at the single nephron level on the same remnant nephrons of Munich-Wistar rats after subtotal NPX to examine the quantitative importance of glomerular sclerosis in relation to proteinuria. In semiquantitative histological examinations, serial thin sections were analyzed so that lesions of glomerular sclerosis in each glomerulus were fully evaluated, avoiding potential errors inherent to the analysis of highly segmental glomerular lesions.

Glossary

C	Protein concentration, grams/deciliter.
θ	Fractional clearance of dextran.
F _{Alb}	Single nephron filtration rate of albumin.
GFR	Glomerular filtration rate (whole kidney inulin clearance rate), milliliters/minute.
K _f	Glomerular capillary ultrafiltration coefficient, nanoliters/(minutes · millimeters of mercury).
MAP	Mean arterial pressure, millimeters of mercury.
NPX	Nephrectomy.
P	Mean pressure, millimeters of mercury.
ΔP	Mean transcapillary hydraulic pressure difference, millimeters of mercury.
π	Colloid osmotic pressure, millimeters of mercury.
Q _A	Initial glomerular plasma flow rate, nanoliters/minute.
R	Resistance to blood flow, millimeters of mercury · minutes/nanoliter.

r_0	Effective radius of small pores, angstroms.
SNFF	Single nephron filtration fraction.
SNGFR	Single nephron glomerular filtration rate, nanoliters/minute.
UprV	Whole kidney protein excretion rate, micrograms/minute.
ω_0	Membrane parameter related to the ratio between the number of large pores versus that of small, selective pores on the glomerular capillary wall.

Subscripts

A	Femoral artery or afferent arteriole.
E	Efferent arteriole.
GC	Glomerular capillary.
T	Proximal tubule.

Methods

Experimental groups

All experiments were performed on adult male Munich-Wistar rats weighing 175–263 g. All animals were allowed free access to regular rat chow and tap water throughout experiments except for the ~ 15 h immediately before micropuncture (groups 1A, 2, and 3) and whole-kidney dextran clearance measurements (groups 2 and 3), when the animals were without food. Table 1 summarizes the specific protocols used in the four experimental groups. 14 rats underwent subtotal NPX. Of these rats, six underwent the assessments of single nephron filtration rate of albumin (F_{Aib}), glomerular capillary hydraulic pressure (P_{GC}), and analysis of functional-histological correlation at the single nephron level 4–6 wk after subtotal NPX (group 1A). Five of the same six rats also underwent histological analysis for the distribution of glomeruli with varying degrees of sclerosis (group 1B). The remaining eight animals (group 2) were subjected to measurements of whole-kidney fractional dextran clearance and micropuncture assessment of the determinants of glomerular sieving function at 1–2 wk after subtotal NPX. A separate group (group 3) of eight age-matched rats that underwent sham surgery served as controls by being subjected to studies identical to those of group 2 animals.

Experimental procedures

Subtotal NPX. 4–6 wk (groups 1A and 1B) or 1–2 wk (group 2) before the study, animals were subjected to subtotal NPX. For this purpose, animals were anesthetized with sodium pentobarbital (Nembutal; Abbott Laboratories, North Chicago, IL; 25–30 mg/kg body wt i.p.), and placed on a temperature-regulated table. All surgical tools were sterilized with 70% ethyl alcohol. Subtotal NPX was performed by right NPX and ligation of two or three main branches of the left renal artery

by silk ligature, to leave approximately one sixth total kidney tissue mass. After the procedures described above, the abdominal incision was closed with 3-0 silk (Ethicon, Inc., Somerville, NJ), and penicillin G (Wyeth Laboratories Inc., Philadelphia, PA; 10,000 U) was injected subcutaneously. When the animals recovered from the anesthesia, they were returned to cages.

Preparatory surgery for micropuncture and dextran clearance measurements. On the day of experiment, animals were anesthetized with Inactin (Byk, Federal Republic of Germany; 100 mg/kg body weight i.p.) and surgically prepared using a procedure routinely performed in our laboratory (7). Briefly, after the tracheostomy, indwelling polyethylene catheters (PE-50; Clay Adams Div., Becton, Dickinson & Co., Parsippany, NJ) were placed into the left and right jugular and left femoral veins for subsequent infusion of plasma, whole blood, inulin, and/or dextran solution. The left femoral artery was also catheterized for monitoring mean arterial pressure (MAP) and for periodic blood collections. MAP was measured by an electronic transducer (model p23Db; Gould Inc., Cleveland, OH) connected to a recorder (model 2200S; Gould Inc.). Laparotomy was then performed. The left ureter was catheterized with a polyethylene tube (PE-10) for subsequent urine collections and the left kidney was immobilized for micropuncture study. To maintain the circulating plasma volume at euolemic level during the experiment, each rat received isooncotic rat plasma in a volume of 10 ml/kg intravenously over the initial 30 min followed by a continuous infusion at the rate of 1.2 ml/kg per h (7). For the estimation of glomerular filtration rate (GFR) and single nephron glomerular filtration rate (SNGFR), 5% inulin in 0.9% NaCl solution was infused intravenously with a priming dose of 0.4 ml, followed by constant infusion at a rate of 1.0 ml/h.

After the above preparatory procedures, rats were subjected to micropuncture and dextran clearance studies specified below. In group 1A and 2 rats, an attempt was made to manipulate the P_{GC} experimentally. After initial micropuncture (groups 1A and 2) and whole-kidney dextran clearance measurements (group 2), rats thus were given verapamil (Searle Pharmaceuticals, Inc., Chicago, IL) intravenously at a rate of 50 μ g/kg per min. After a 30-min equilibration period, with MAP having reached a steady state level, micropuncture and dextran clearance studies were repeated.

Measurement of F_{Aib} (group 1A: 4–6 wk after NPX). Pairs of surface glomeruli and the earliest segment of proximal tubules originating from these glomeruli were identified by injecting (with a pipette of 2–4 μ m tip diameter), with modest pressure, a small quantity of 0.1% lissamine green into proximal convolutions in the vicinity of surface glomeruli as described elsewhere (8). Because of the removal of two-thirds tissue mass from the remnant kidney during the subtotal nephrectomy, each rat had only < 10 surface glomeruli. Of these, approximately half did not have the earliest segment of proximal tubules on the surface.

Precisely timed (1–2 min) samples of fluid were collected from the earliest surface segment of proximal tubules previously identified for determination of SNGFR and F_{Aib} . For the purpose of this timed fluid collection, mineral oil stained with Sudan black was injected into the earliest proximal tubule with a collection micropipette (with outer tip diameter of 6–8 μ m) to fill ~ 3–5 diameters length of the tubule lumen. Fluid was collected with the minimum degree of suction required to prevent the oil block from flowing downstream. This measurement has recently been shown to provide an accurate estimated value for SNGFR in remnant nephrons after subtotal NPX (8).

After the final micropuncture measurements, a small volume of dye (The Davidson Marking System; Bradley Products, Inc., Bloomington, MN) was injected into the subcapsular space just above, and/or into Bowman's space of the surface glomeruli on which micropuncture measurements were performed, to identify them during subsequent histological study.

Micropuncture measurement of the determinants for glomerular sieving function (group 2: 1–2 wk after NPX and group 3: sham-operated control). Using the method previously described in detail (7, 9, 10), micropuncture measurements and collections were made in all group 2 animals to determine SNGFR, P_{GC} and mean proximal tubule

Table 1. Protocol Used in Groups 1A, 1B, 2, and 3

	Parameters measured	Experimental period
Group 1 (4–6 wk after subtotal nephrectomy, $n = 6$)		
Group 1A ($n = 6$)	SNGFR, F_{Aib} , P_{GC} , semiquantitation of glomerular sclerosis	Before and during verapamil administration
Group 1B ($n = 5$)	Histogram of glomeruli with various degrees of glomerular sclerosis	No functional assessment
Group 2 (1–2 wk after subtotal nephrectomy, $n = 8$)		
	Determinants for glomerular sieving function, fractional clearance of dextran	Before and during verapamil administration
Group 3 (1–2 wk after sham operation, $n = 8$)		
	Determinants for glomerular sieving function and fractional clearance of dextran	Baseline measurement only

hydraulic pressure (P_T), femoral arterial (C_A) and efferent arteriolar (C_E) plasma protein concentrations, single nephron filtration fraction (SNFF), initial glomerular plasma flow rate (Q_A), and glomerular capillary ultrafiltration coefficient (K_f), as well as resistances of single afferent (R_A) and efferent (R_E) arterioles. Colloid osmotic pressures (π) of plasma entering (π_A) and leaving (π_E) glomerular capillaries were estimated from C_A and C_E by using the equation derived by Deen et al. (9).

In addition to these micropuncture measurements, timed urine samples were taken at each experimental period for measurement of urine protein excretion rate (UprV) and whole kidney GFR. For this purpose, blood samples also were taken from the femoral arterial catheter at the beginning and the end of each experimental period. These measurements were completed within ~ 20 min, and followed immediately by the dextran clearance measurement specified below.

Dextran clearance measurement (group 2: 1–2 wk after NPX and group 3: sham-operated control). Fractionated dextran with average molecular mass of 10(T-10), 40(T-40), and 70(T-70) kD was purchased from Pharmacia Fine Chemicals (Piscataway, NJ). A 20-mg/ml solution containing 50.0% T-70, 37.5% T-40, and 12.5% T-10 was oxidized with NaI_3 at pH 5.0 and reacted with tyramine in a borate buffer at pH 9.0. The tyraminil-dextran was separated from unbound reactants by gel filtration on a Sephadex G-25 column (total volume $V_T = 50$ ml) (Pharmacia Fine Chemicals). The purified mixture was radiolabeled at pH 7.4 with Iodo-Beads (Pierce Chemical Co., Rockford, IL) and I-125 (New England Nuclear, Boston, MA). Unreacted I-125 was removed by gel chromatography on a short disposable Sephadex G-25 column ($V_T = 10$ ml). The ionic strength and pH of the solution were adjusted, and the mixture was sterilized by filtration and stored at 4°C. The iodinated dextran solutions were used within 7 d of the date of preparation.

The dextran clearance study was performed immediately after the micropuncture procedures. At the beginning of each dextran clearance measurement, the transit time was determined by intravenous injection of 0.2 ml of lissamine green solution. In each experimental period, 0.2 ml of the I-125 dextran solution ($\approx 40,000$ cpm/ μl) was injected intravenously, followed by a constant infusion at the rate of 0.034 ml/min. Approximately 5 min after completing the priming injection, a continuous collection of blood was started from the femoral artery for 20 min at a rate of 0.034 ml/min, using a withdrawal/infusion pump (model 941, Harvard Apparatus Co., S. Natick, MA). Simultaneously with the withdrawal/infusion pump, fresh whole blood collected from a littermate was transfused to replace, volume-to-volume, the blood withdrawn. Urine was collected from the left ureteral catheter for an equivalent time period corrected for the transit time. The blood samples were immediately centrifuged and plasma and urine aliquots were separated for subsequent analysis.

The fractionation of urine and plasma samples containing dextrans of graded molecular size and the measurement of radioactivity of each size of dextran were performed as previously described (11–13). Briefly, separation of dextrans into narrow (2 Å) fractions was accomplished by gel permeation chromatography using a column ($V_T = 200$ ml, length = 40 cm) packed with an even mixture of acrylamide-agarose, AcA 34, and 44 (LKB Instruments Inc., Paramus, NJ). Radioactivity of each fraction of dextran (≈ 1.6 ml) was then measured in a gamma counter (1282 CompuGamma; LKB Wallac, Turku, Finland).

Analytical. Plasma and urine concentrations of inulin were determined by the macroanthrone method (14). Details of the analytical procedures for inulin determination in nanoliter samples, and C_A and C_E measurements are given elsewhere (15, 16). The volume of fluid collected from individual proximal tubules by micropuncture study in groups 1A and 2 was estimated from the length of the fluid column in a constant-bore capillary tube of known internal diameter. The urine protein concentration was measured by the Coomassie Brilliant Blue method (17).

The concentration of albumin in tubule fluid obtained by micropuncture was determined by solid phase ELISA using a double-antibody sandwich technique (18). After measurement of the volume collected, tubule fluid samples were transferred directly into aliquots of

either 300 or 600 μl of a 0.025 M EDTA, pH 7.3 buffer solution containing 2 mg/ml of human IgG (Armour Pharmaceutical Co., Tarrytown, NY) and 0.05% Tween 20 (Fisher Scientific Co., Pittsburgh, PA) and were stored at -20°C until assayed.

Quantitative ELISA for rat albumin in concentrations from 1 to 20 ng/ml was performed using sample volumes of either 50 or 100 μl /well. For the measurement of tubular fluid albumin in samples that had been diluted in 600 μl of the blocking buffer described above, polyvinyl chloride 96-well, flat-bottomed microtiter plates (Dynatech Laboratories, Inc., Alexandria, VA) were coated with an IgG fraction of affinity-purified rabbit anti-rat albumin (5 $\mu\text{g}/\text{ml}$) in 0.025 M EDTA buffer, pH 9.3 (100 μl /well) for 15 h at 4°C. Wells were washed three times (200 μl /well) with PBS (0.15 M NaCl and 0.02 M NaH_2PO_4 , pH 7.3) containing 0.05% Tween 20 (PBS-Tween) followed by incubation with the blocking buffer (200 μl /well) for 30 min at 37°C. Rat albumin (Miles Laboratories, Inc., Naperville, IL) standards containing 1–20 ng/ml, and samples obtained by micropuncture and diluted in blocking buffer, were incubated for 60 min at 37°C in triplicate (100 μl /well). After being washed three times with PBS-Tween, a 1:6,400 dilution of peroxidase-conjugated IgG fraction of sheep anti-rat albumin (Cooper Biomedicals, Inc., Malvern, PA) in blocking buffer (100 μl /well) was incubated for 60 minutes at 37°C. After being rewashed six times with PBS-Tween, the substrate reaction using 0.137% *o*-phenylenediamine (Aldrich Chemicals Co., Milwaukee, WI), 0.009% H_2O_2 in 0.2 M Tris/HCl, 0.15 M NaCl buffer, pH 6.0 (100 μl /well) was performed in the dark for 60 min at room temperature. The reaction was stopped with 0.1 M sodium sulfite in 4 N sulfuric acid (50 μl /well). Optical densities were determined at 490 nm (with reference OD of 570 nm) using a dual wavelength mode microtiter plate reader (model MR 580, Dynatech Laboratories, Inc.) that automatically subtracts the background OD of the substrate reaction blank.

Samples that exceeded the concentration of 20 ng/ml were identified by preliminary measurement performed in duplicate. These samples were further diluted (usually two- or threefold) with blocking buffer as required before assay in triplicate. The selection of buffer volume for initial direct tubular fluid dilution in each group of rats was based on the anticipated magnitude of proteinuria. To measure samples that had been diluted in 300 μl of blocking buffer, the volumes applied in each step were halved (i.e., 50 μl of sample/well). The concentrations in individual samples were determined by plotting the mean OD of the triplicate determinations against a curve derived from standards run on the same plate. A representative standard curve is shown in Fig. 1. The correlation coefficients of the simple regression lines for standards derived for assays using 100- μl samples/well and using 50- μl samples/well indicate that these volumes are equally satisfactory for quantitative analysis of rat albumin ($r > 0.998$ in both cases). This ELISA system detected < 0.1 ng albumin/100 μl sample.

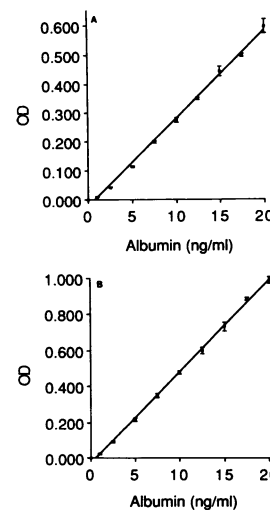


Figure 1. (A) Representative ELISA for rat albumin standards using 100- μl samples per well in triplicate (mean \pm SD). $y = -0.0271 + 0.0510x$ ($r = 0.999$). (B) Representative ELISA for rat albumin standards using 50- μl samples per well in triplicate (mean \pm SD). $y = -0.0232 + 0.0304x$ ($r = 0.998$).

To examine the reproducibility of the collection and assay for the tubular albumin concentration, a separate group (i.e., separate from groups 1–3 experimental rats) of three normal control rats and three rats subjected to subtotal NPX 4–6 wk earlier were examined as follows: after surgical preparation as in group 1, collections of earliest proximal tubular fluid were performed for albumin assay twice consecutively from the same tubules. Linear regression analysis for the duplicates ($n = 10$ duplicates) from this study showed $r = 0.806$, $P < 0.05$. Probability of the slope (0.694) and the intercept (0.493) were 1 and 0, respectively, which were calculated to be statistically significant ($P < 0.025$ and $P < 0.05$, respectively). Therefore, our methods for collection and assay for determining F_{Alb} were shown to be highly reproducible.

Calculations of glomerular hemodynamic and membrane parameters. Based on the data obtained from micropuncture studies, SNGFR, SNFF, π_A , π_E , Q_A , R_A , R_E , mean glomerular transcapillary hydraulic pressure difference (ΔP) and K_f were calculated using previously published equations (7, 9). Fractional clearances of graded-size dextrans (θ) were calculated using the equation: $\theta = (U/P)_{Dextran}/(U/P)_{Inulin}$, where $(U/P)_{Dextran}$ and $(U/P)_{Inulin}$ refer to the urine-to-plasma ratio of dextrans and inulin, respectively.

To assess the glomerular membrane permeability characteristics for macromolecular transport, two membrane parameters defined in the mathematical model of Deen et al. (19) were calculated. This model postulates two functionally distinct pathways for movement of macromolecules across the capillary wall. One of the pathways consists of small pores of radius r_0 , which predominates and serves as the major pathway for water and small molecules, whereas the other pathway contains pores that are few in number, but sufficiently large in radius that they exhibit negligible selectivity even for the largest dextrans studied (molecular radius 60 Å). The contribution of the nonselective shunt pathway is characterized by a parameter ω_0 , which is related to the fraction of filtrate volume passing through these large pores. Specifically, ω_0 is the theoretical fraction of volume flow that would take place through the large pores if all pores experienced the same net driving pressure. The actual fraction of filtrate volume passing through the postulated shunt (ω) is larger than ω_0 and varies according to the position along the capillary, because flow through the small pores is opposed by the colloid osmotic pressure of capillary plasma (protein reflection coefficient near unity), whereas that through the large pores of the shunt is not (reflection coefficient near zero). Local colloid osmotic pressure, in turn, is modulated by ΔP , Q_A , and other hemodynamic parameters. Whereas values for ω are affected by these parameters, ω_0 thus is independent of these effects and solely reflects the characteristics of the capillary wall per se (19). Computation of r_0 and ω_0 was performed using mean values of C_A , Q_A , ΔP , K_f , and θ of each group. The mathematical details of the model used, and the assumptions on which it is based, have been presented in detail elsewhere (19).

Histological study. Histological studies were performed by light microscopy at the completion of micropuncture in group 1 rats. Kidneys were removed and fixed in 10% neutral buffered formalin. In the kidneys obtained from group 1A, the location of each specific glomerulus subjected to micropuncture was readily identified by the dye spot injected before harvesting the kidney. Serial 3- μ m-thick sections were made and stained with periodic acid-Schiff. A semiquantitative score (sclerosis index) was used to evaluate the degree of glomerular sclerosis in these glomeruli, using the method of Raij et al. (20). A minimum of 10 sections displaying even distribution throughout each glomerulus were examined, and the severity of sclerosis was graded from 0 to 4+ for each section. The 1+ lesion represented involvement of < 25% of the glomerulus, whereas 4+ reflected 75–100% of the glomerulus. A single score was then obtained for each glomerulus by averaging the scores from these multiple sections. In separate groups of rats (group 1B), population distributions of varying degree of glomerular sclerosis were examined 4–6 wk after subtotal NPX. For this purpose, the degree of glomerular sclerosis was determined for 169 randomly selected glomeruli (obtained from five rats) in group 1B rats, using the above described semiquantitative scoring scale applied on multiple thin sections per glomerulus.

Statistics. Results are expressed as mean \pm SE. Differences of data among groups 1, 2, and 3 were tested using analysis of variance with Bonferroni's method for comparing multiple groups (21). The t test was used for the intergroup and within-group comparisons of hemodynamic and dextran clearance data. Linear regression analysis and analysis of covariance were used to examine the correlation between the sclerosis index versus F_{Alb} (22). The results were denoted as statistically significant when the P value was < 0.05 .

Results

Systemic and whole kidney parameters during early and late stages in subtotal nephrectomized rats

Comparisons between the baseline values of group 1A and 2 vs. group 3 normal control rats. Systemic and whole kidney data obtained from groups 1A, 2, and 3 at baseline are shown in Table II. As illustrated, when compared with group 3 sham-operated control rats, animals 1–2 wk after subtotal NPX (group 2) had modest systemic hypertension, proteinuria, and decreased whole kidney GFR. The average value of MAP in group 2 rats thus was significantly higher than that in group 3 rats (131 ± 3 vs. 113 ± 2 mmHg, $P < 0.005$). Group 2 subtotal nephrectomized rats also had significant elevation in urine protein excretion rate (27 ± 1 vs. 8 ± 1 μ g/min, $P < 0.005$). GFR was significantly reduced in group 2 (0.65 ± 0.08 ml/min) compared with group 3 (1.04 ± 0.06 ml/min). Essentially identical patterns were also seen in group 1A animals, which were studied 4–6 wk after subtotal NPX. However, systemic hypertension and reduction in GFR were more marked in this group (Table II).

Glomerular function and structure in remnant nephrons during late stages

Correlation during the baseline condition in subtotal nephrectomized rats (groups 1A and 1B). The relationship between the sclerosis index and albumin filtration rate, determined for each glomerulus in group 1A rats, is demonstrated

Table II. Summary of Data for Whole Body and Kidney Data in Group 1A, 2, and 3 Animals

	Body wt	MAP	UprV	GFR
	g	mmHg	μ g/min	ml/min
Group 1A (4–6 wk after subtotal NPX, $n = 6$)				
Baseline	188	172*	52*	0.42*
	± 11	9	14	0.06
Intravenous verapamil	—	100 [†]	31 [†]	0.44
		3	7	0.06
Group 2 (1–2 wk after subtotal NPX, $n = 8$)				
Baseline	220	131*	27*	0.65*
	8	3	1	0.08
Intravenous verapamil	—	84 [†]	14 [†]	0.52
		4	2	0.10
Group 3 (normal controls, $n = 8$)				
	231	113	8	1.04
	6	2	1	0.06

Values are expressed as mean \pm SEM.

Values show statistically significant ($P < 0.05$) difference from those of group 3 (*), or from baseline within the same group ([†]) by analysis of variance followed by multigroup comparison of the Bonferroni method and the paired t test, respectively.

in Fig. 2. Each point represents the data from a single glomerulus. Clearly, no correlation was seen between these functional and histological parameters ($r = 0.022$, $P > 0.25$). The ELISA developed for these studies provided an assay range from 1 to 20 ng rat albumin/ml. The relatively broad range and the sensitivity of this assay thus allows the concentrations of albumin in samples obtained by micropuncture to be precisely measured. Others have recently shown assays for human albumin by ELISA with sensitivity comparable to our assay to be reliable and reproducible (23–26). The values determined by ELISA were closely correlated with those obtained by other assays such as RIA (24) or radial immunodiffusion (25, 26). Potential factors that might skew results of albumin determinations in samples obtained by micropuncture include contamination by plasma and tissue fluids and loss of albumin during processing. As described in Methods, our analysis of paired samples of the earliest proximal tubule fluid from the same nephrons showed the coefficient of variation of albumin concentration in these paired samples to be remarkably low. Our ELISA method detects < 1 ng/ml albumin and provides a slightly more sensitive assay system than the ultramicrodisc gel electrophoresis technique that has been used for the measurement of albumin in tubular fluid (27).

In group 1B rats, which were prepared in a fashion similar to that of group 1A rats, we examined the population distribution of glomeruli with varying degrees of sclerosis index, which were obtained from multiple thin section analyses. The typical glomerular morphology seen in the examined kidneys is illustrated in Fig. 3 A. Among the glomeruli seen in the picture, five of the glomeruli have no sclerosis with a segmental lesion in one glomerulus. The same distribution pattern of sclerosis was observed in the glomeruli from five group 1B-kidneys examined. As shown in Fig. 3 B, even at the stage of 4–6 wk after subtotal NPX, the majority of glomeruli had a minimal degree of sclerosis.

Effect of verapamil administration. Verapamil infusion in groups 1A and 2 rats resulted in a decrease in MAP and UprV without any effect on GFR (Table II). Thus, MAP decreased some 40% in group 1A ($P < 0.005$). UprV also decreased from 52 ± 14 to 31 ± 7 $\mu\text{g}/\text{min}$ in group 1A ($P < 0.05$). The P_{GC} in nine glomeruli before and during verapamil administration in remnant nephrons of group 1A animals showed a marked reduction, from 70 ± 5 to 50 ± 3 mmHg during verapamil infusion ($P < 0.005$). This reduction was greater in glomeruli that had markedly high P_{GC} levels under baseline conditions, so that the P_{GC} of virtually all of the glomeruli fell to a range near the normal control level of group 3 animals. As shown in Fig. 4, despite this reduction in P_{GC} , SNGFR values measured in most nephrons were found to be essentially unaffected by verapamil administration ($P > 0.1$). In contrast, F_{Alb} measured in

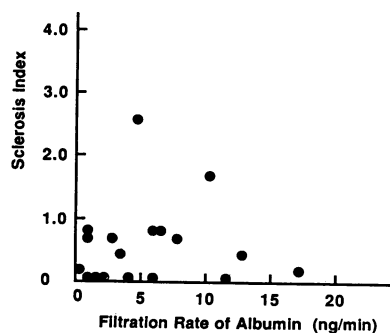


Figure 2. Relationship between sclerosis index and albumin filtration rate in 18 glomeruli of group 1A subtotal nephrectomized rats ($n = 6$) ($r = 0.022$, $P > 0.25$).

these nephrons, decreased in all nephrons examined (Fig. 4) ($P < 0.005$). The sclerosis index of these 11 glomeruli was 0.15 ± 0.09 .

Glomerular hemodynamics and sieving function in intact remnant nephrons during early stages

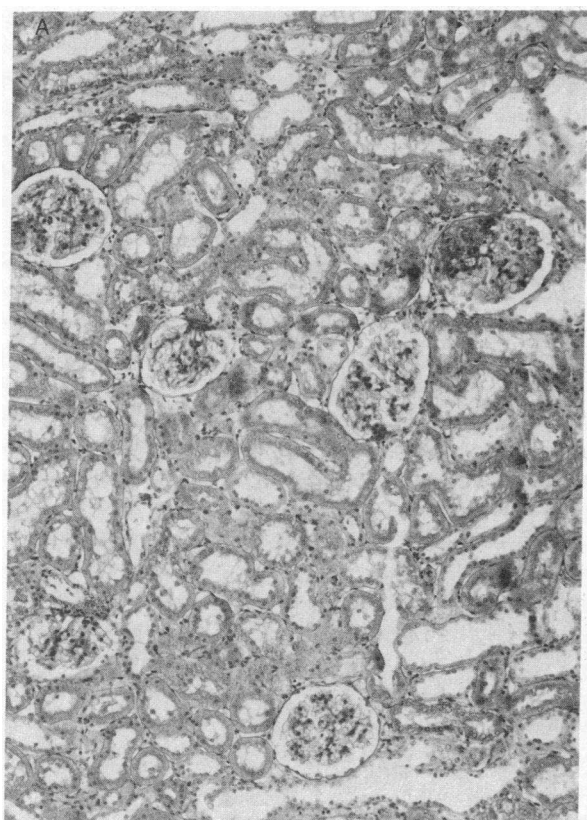
Glomerular hemodynamics: comparisons between the baseline values of subtotal nephrectomized (group 2) and normal control rats (group 3). Average values for several pertinent measurements of single nephron function in group 2 and 3 animals are summarized in Table III. The remnant nephrons of group 2 rats are characterized by marked glomerular hyperfiltration and perfusion. Values for SNGFR and Q_A in group 2 (76.1 ± 5.8 and 226 ± 12 nl/min, respectively) were significantly higher than those in group 3 (41.2 ± 1.0 and 142 ± 9 nl/min, respectively, $P < 0.005$). The remnant nephrons of group 2 rats also had significantly elevated P_{GC} , averaging 65 ± 3 mmHg, compared with those (45 ± 1 mmHg) measured in group 3 ($P < 0.01$). Likewise, values of ΔP in group 2 were elevated over group 3 control levels (52 ± 3 vs. 34 ± 1 mmHg, $P < 0.005$). In contrast to these abnormally high pressure levels, group 2 animals were characterized by substantially depressed values for K_f , averaging 2.36 ± 0.29 nl/(min \cdot mmHg), compared with 3.63 ± 0.16 nl/(min \cdot mmHg) obtained in group 3 controls ($P < 0.05$). It is clear from Table III that the high P_{GC} values in group 2 largely resulted from an elevation in R_E and a decrease in R_A in this group. The observed patterns of glomerular hypertension, hyperperfusion, and hyperfiltration in remnant nephrons are essentially identical to those reported by a number of investigators (5, 23). Although distribution patterns of sclerosis in these animals were similar to those in group 1B (4–6 wk after subtotal NPX, Fig. 3 B) animals, glomeruli at the earlier stage were more homogenous and less sclerotic.¹

Glomerular hemodynamics: effect of verapamil administration in group 2 rats. As shown in Table III and Fig. 5, during administration of verapamil in group 2 rats, values for SNGFR remained essentially unchanged. In contrast, values for P_{GC} (45 ± 3 mmHg), and ΔP (34 ± 1 mmHg) during verapamil infusion, were shown to be significantly depressed to levels similar to those measured in group 3 normal control rats. In contrast, values for Q_A (296 ± 18 nl/min) were further increased by verapamil infusion, by some 30% on average. Calculation of arteriolar resistances revealed that values for both R_A and R_E during verapamil infusion in group 2 were depressed below group 2 baseline (preinfusion) levels.

Glomerular sieving function: comparisons between the baseline values of subtotal nephrectomized (group 2) and normal control rats (group 3), and effect of verapamil administration in group 2 rats. The results of fractional dextran clearance (θ) measurements in group 2 and 3 animals are summarized in Fig. 6. As shown, for group 3 normal control rats, θ was shown to decrease progressively as the size of dextran molecules increased, reflecting the size-selective barrier function of the glomerular capillary wall. The baseline condition of group 2 subtotal nephrectomized rats was characterized by significantly ($P < 0.05$) enhanced θ for molecular radii $> 36 \text{ \AA}$, when compared with group 3 normal control rats.

Administration of verapamil, which depressed ΔP and caused diminution of urine protein excretion rate (from 27 ± 1

1. The population of glomeruli with sclerosis index < 0.1 in group 2 (61% of 99 glomeruli examined) was significantly ($P < 0.05$ by Chi square test) greater than that in group 1B (40%).



NUMBER OF GLOMERULI

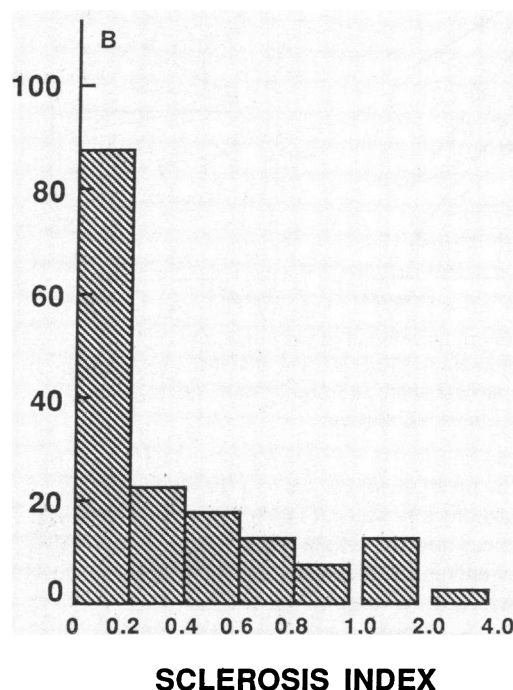


Figure 3. (A) Photomicrograph ($\times 160$) of the glomeruli obtained from a kidney of group 1B (4–6 wk after subtotal NPX). One glomerulus shown on the top right exhibits mild focal sclerosis, whereas the other five glomeruli shown have little or no sclerosis. (B) Histo-

gram showing distribution of glomeruli with different degrees of sclerosis. The data is based on 169 glomeruli harvested from five kidneys 4–6 wk after subtotal NPX (group 1B).

to $14 \pm 2 \mu\text{g}/\text{min}$, $P < 0.05$) in group 2 rats, was also shown to bring about a shift of θ values for higher molecular size dextrans toward the values observed in group 3 normal control animals. Values of θ for dextran molecular radii $> 42 \text{ \AA}$ thus were significantly ($P < 0.05$) lower than those obtained in group 2 baseline values (Fig. 6).

Using the mathematical model of Deen et al. (19), membrane parameters that determine the macromolecule fluxes across the glomerular capillary wall were calculated for group 2 and 3 rats. The results are shown in Figs. 7-A and B. As shown in Fig. 7 A, between group 2 (baseline) and group 3, a modest difference was seen in the calculated values for r_0 (54.4 and 48.3 \AA , respectively), the radius of small selective pores comprising the bulk of the membrane. A marked difference between these two groups was noted in the value for ω_0 , the parameter related to the fraction of filtrate passing through large nonselective pores. As shown in Fig. 7 B, ω_0 was 1.35×10^{-4} in group 3 normal control and 34.1×10^{-4} in group 2 subtotally nephrectomized rats under baseline conditions. A substantial decrease in this parameter was seen during verapamil-induced reduction in ΔP (Fig. 7 B), the value of ω_0 averaging 12.8×10^{-4} (group 2, verapamil), whereas the value for r_0 was essentially unaffected (Fig. 7 A).

Discussion

The remnant glomeruli of rats that were subtotally nephrectomized several weeks earlier have been shown to be character-

ized by highly heterogeneous function and structure (3–5, 8). In this study, we found that nephrons without glomerular sclerosis (i.e., with intact structure at a light microscopic level) often had the highest filtration rate of albumin (Fig. 2). The contribution to proteinuria of glomeruli with a particular histological pattern depends not only on the amount of protein filtered by the individual glomeruli, but also on the proportion of glomeruli with this pattern. We thus determined the distribution of glomeruli with varying degrees of sclerosis, which were obtained in the same kidneys subjected to the assessment of glomerular functional-histological correlation (group 1B). Even 4–6 wk after subtotal NPX, when azotemia and marked proteinuria were evident, many of the glomeruli were still nonsclerotic (Fig. 3). Collectively, our results are taken to indicate that nonsclerotic glomeruli are primarily responsible for the proteinuria in this model. It thus is unlikely that the development of glomerular sclerosis per se in the course of progressive renal disease is linked to the development of proteinuria. Instead, our observations are in accordance with the decrease in proteinuria at the advanced stage of chronic renal disease when sclerotic glomeruli predominate (28, 29).²

2. Theoretically, severely sclerotic glomeruli could contribute to the proteinuria proportionally to a greater extent than that presumable from their protein filtration rate via reduced tubular reabsorption. However, our observation that the population of such glomeruli was far less than that of nonsclerotic glomeruli makes it unrealistic that those sclerotic glomeruli exert a greater influence on the proteinuria than the intact glomeruli.

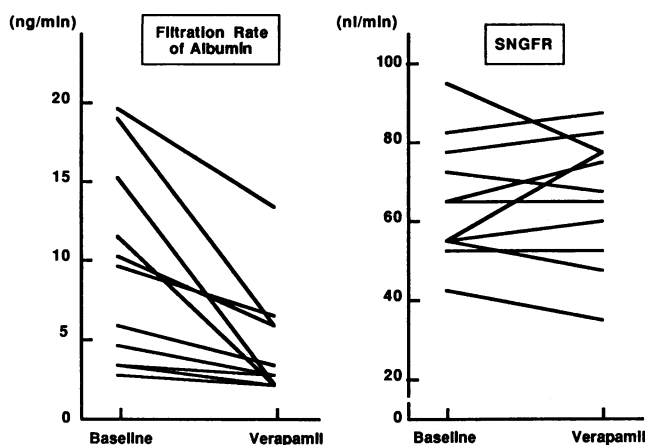


Figure 4. Effect of normalization of mean glomerular capillary pressure in group 1A animals, on F_{Aib} (left) and SNGFR (right). Each single line represents data obtained from the same single glomerulus before and during verapamil infusion.

To explore the mechanism underlying the sieving defect of these relatively structurally well-preserved nephrons found at a later stage, we measured the whole-kidney sieving coefficient using polydispersed neutral dextrans and glomerular microcirculatory dynamics by micropuncture shortly (i.e., 1–2 wk) after subtotal NPX. Remnant kidneys studied shortly after subtotal NPX have a relatively homogenous population of hyperfiltering glomeruli that are morphologically similar, in many respects, to the histologically intact glomeruli of the later phase (8). Under these circumstances, the measured whole-kidney sieving coefficient can be regarded as representative of each single glomerulus.³ As described in Results, the sieving coefficients of these kidneys for large dextrans were somewhat selectively increased ($r > 36 \text{ \AA}$, $P < 0.05$). A similar defect in glomerular size selective function has been previously documented in a similar rat model (6)⁴ and also in some chronic forms of human primary glomerulopathy (1, 2).

We have previously demonstrated in rat models of renal vein obstruction (12) and glomerulonephritis (13) that acute upward or downward changes in glomerular capillary hydraulic pressure induced parallel changes in urine protein excretion rate. In those studies, P_{GC} was either acutely or chronically elevated in Munich-Wistar rats, and subsequently returned to near baseline levels by infusion of an angiotensin II antagonist, saralasin, or a renal vasodilator, acetylcholine. Moreover, in both studies, the changes in the urinary protein excretion rate were also accompanied by parallel changes in fractional clear-

ances of large dextrans (12, 13). In this study, we found P_{GC} to be markedly elevated in the intact remnant glomeruli, as previously documented by others (5, 30). We therefore attempted to ascertain the causal relationship between this high P_{GC} and the degree of sieving defect in these nephrons. In designing the protocol, we felt that this experimental goal could best be accomplished by manipulating P_{GC} by infusion of a pharmacological agent in a dose that does not cause changes in fluid flux across the glomerular capillary wall to avoid changes in the convective force-dependent macromolecule filtration rates. Verapamil infusion in group 2 animals thus successfully returned P_{GC} values from the abnormally high baseline levels to near normal control levels (Fig. 5). There was a simultaneous decrease in urinary protein excretion (Fig. 5) and fractional clearances of larger dextran molecules (Fig. 6). This pattern of P_{GC} -sensitive changes in glomerular sieving function is the same as that observed in rat models of renal vein constriction (12) and glomerulonephritis (13).

To test more directly whether the prevailing high glomerular pressure is indeed a major cause of the sieving defect of the intact glomeruli at the late phase of the disease, we assessed the filtration rate of albumin at the single nephron level before and during experimental normalization of glomerular capillary pressure by intravenous infusion of verapamil. These glomeruli without sclerosis displayed uniformly elevated P_{GC} and filtration rate of albumin during baseline measurements. In response to the normalization of glomerular capillary pressure, the filtration rate of albumin declined significantly in these nephrons, whereas SNGFR remained essentially constant (Fig. 4), thus supporting the notion that the sieving defect seen in the chronic phase of this model is under the major influence of the prevailing high glomerular capillary pressure in structurally relatively well-preserved nephrons.⁵

To determine whether the close association observed between P_{GC} and macromolecule filtration was simply the result of effects on the convective and/or diffusive driving forces acting on the glomerular capillary wall, or of alterations in the barrier properties of the wall per se, we used a mathematical model (19) to calculate membrane parameters from the clearance and micropuncture data. According to this model, which has been successful in correlating dextran sieving data in several forms of glomerular injury (2, 12, 13, 19, 31), glomerular size selectivity is characterized by two parameters, r_0 and ω_0 . Our calculations revealed that during each of our experimental manipulations (induction of high P_{GC} in remnant nephrons and infusion of verapamil), changes in P_{GC} were accompanied by parallel changes in the fraction of filtrate volume transported through large, nonselective pores (related to ω_0), whereas the pore radius of the predominant pathway for water, r_0 , remained essentially unchanged.⁶ On the basis of these mathematical analyses, in Fig. 8, we schematically present the hypothetical changes occurring in the glomerular capillary

3. Moreover, the measurements and computation of various indices for single glomerular dynamics are performed based on the micropuncture data obtained from different nephrons. The existence of heterogeneity of function among nephrons, therefore, precludes meaningful assessment of single glomerular function. Furthermore, the ability to compute membrane parameters for glomerular size-selective function in kidneys with heterogenous nephron injuries is severely limited, since the computation uses the whole kidney values, and glomerular hemodynamic data obtained by micropuncture, as input values.

4. Olson et al. (6) previously documented that subtotal NPX, which was more extensive than that of our models, was characterized by the loss of both glomerular size-selective and charge-selective function. In this study, we only examined the underlying mechanism(s) of the defect in size selectivity.

5. We did not measure P_{GC} and F_{Aib} from the same glomeruli, since micropuncture measurement of P_{GC} causes albumin leak, and this makes it virtually impossible to perform subsequent F_{Aib} determination. For this reason, we assessed these two parameters in two separate groups of glomeruli, with a similar sclerosis index.

6. As the computation of membrane parameters was made by using mean values obtained by pertinent micropuncture and whole kidney measurements in each experimental group, no statistical evaluation was made for the analysis of the differences in membrane parameters among experimental groups.

Table III. Summary of Various Glomerular Microcirculatory Parameters in Group 2 and 3 Animals

	SNGFR	P_{GC}	ΔP	C_A	Q_A	R_A	R_E	K_f	SNFF
	nl/min	mmHg	mmHg	g/dl	nl/min	mmHg·min/nl	mmHg·min/nl	nl·mmHg/min	
Group 2 (1–2 weeks after subtotal NPX, $n = 8$)									
Baseline	76.1*	65*	52*	5.4	226*	0.156*	0.143*	2.36*	0.34
	± 5.8	3	3	0.1	12	0.010	0.009	0.29	0.02
	68.0	45 [†]	34 [†]	5.3	296	0.074	0.064 [†]	3.27 [†]	0.24 [†]
Intravenous verapamil	6.0	3	1	0.1	18	0.004	0.004	0.33	0.03
Group 3 (sham-operated control, $n = 8$)									
	41.2	45	34	5.6	142	0.275	0.115	3.63	0.30
	1.0	1	1	0.1	9	0.020	0.009	0.16	0.02

Values are expressed as mean \pm SEM. Efferent arteriolar colloid osmotic pressure-to-glomerular transcapillary hydraulic pressure difference ratio was found to be <1.0 in two group 3 rats. In these animals, unique K_f values were calculated and pooled with minimum K_f values to obtain average values. Values show statistically significant ($P < 0.05$) difference from those of group 3 (*), or group 2 baseline period ([†]) by unpaired and paired t test, respectively.

which reflect an increased ratio between the number of large pores versus small pores. Note that the increase in the relative quantity of large pores, although having little influence on fluid flux due to their essentially negligible population when

compared with that of small pores, exerts a profound influence upon transcapillary macromolecular transport, since in both normal and disease states, the large pores are essentially the sole channels for the largest macromolecules to reach the urinary space. The close association between P_{GC} and ω_0 observed in this study has been reported previously in other experimental manipulations (12, 13). These findings are consistent with the view that there is an ultrastructural defect of the glomerular capillary wall of the light microscopically intact glomeruli, which accounts for the observed marked increase in ω_0 .

In summary, we obtained evidence to indicate that, in the rat model of subtotal NPX, glomeruli without major histological changes, or "intact nephrons," are primarily responsible for the proteinuria. Obviously, more subtle changes, such as surface alterations of the epithelial cells, that can be demonstrated only by electron microscopic study, may better correlate with the degree of sieving dysfunction at the single glomerular level. In morphologic studies of renal tissue from patients with nephrotic syndrome and focal segmental glomerular sclerosis, extensive ultrastructural changes of epithelial cell foot process effacement are typically not confined

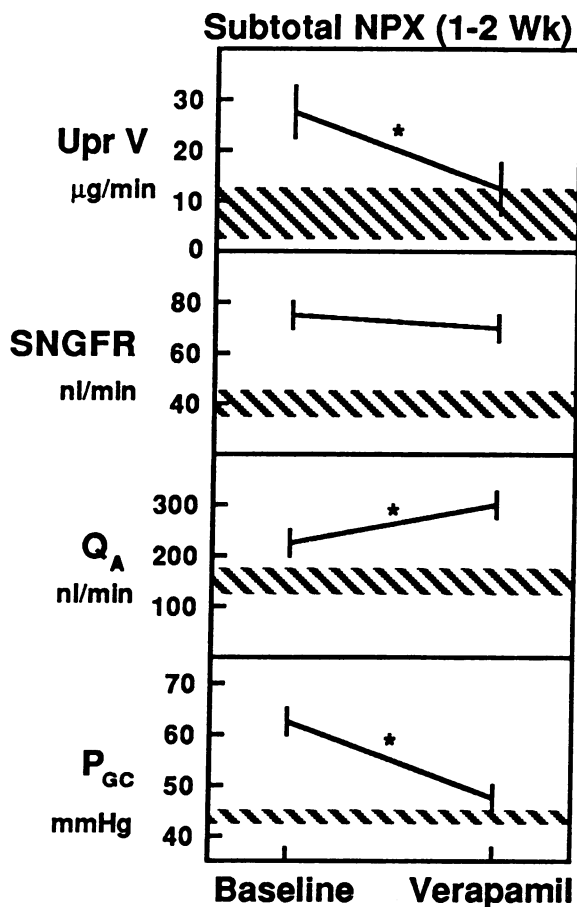


Figure 5. Changes in glomerular microcirculatory hemodynamic parameters and urine protein excretion rate before and during verapamil infusion in group 2 subtotal nephrectomized rats. ± 1 SE of mean values from normal control rats (group 3) are represented by the shaded zones. *denotes statistically significant ($P < 0.05$) change between the study periods.

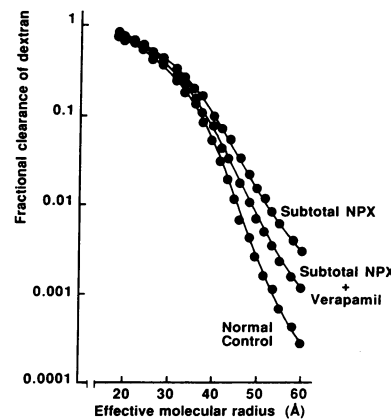


Figure 6. Comparison of data for fractional clearance (θ) of graded size dextrans obtained from group 2 (1–2 wk after subtotal NPX) and 3 (sham-operated) animals. In group 2 rats undergoing baseline conditions (subtotal NPX), θ values for molecular radii $> 36 \text{ \AA}$ were significantly ($P < 0.05$) higher than in group 3 normal control rats (normal control).

In group 2 rats given continuous infusion of verapamil (subtotal NPX + verapamil), θ values for molecular radii $> 42 \text{ \AA}$ were significantly lower ($P < 0.05$) than those obtained in baseline conditions from the same group. However, these values in group 2 using verapamil were still higher than those found in group 3.

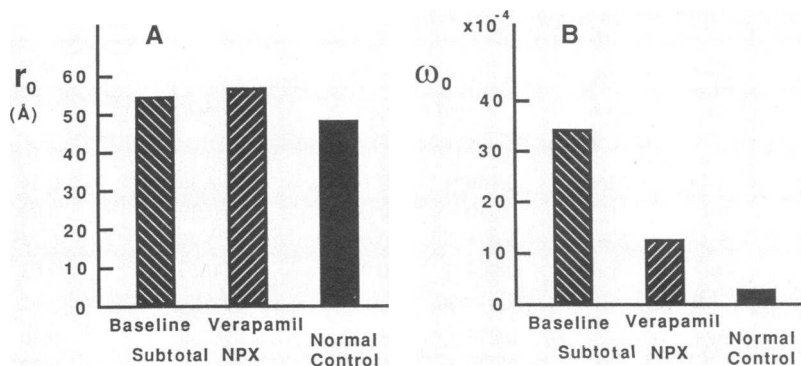


Figure 7. Comparison of calculated values for membrane parameters among group 2 and 3 animals. (A) Radii of small selective pores (r_0) were virtually indistinguishable between groups and conditions. (B) In contrast, the index for fractional volume flux through large nonselective pores (ω_0) was markedly increased in group 2 baseline (left) compared with group 3 (right), and those obtained from group 2 during verapamil infusion (middle) were markedly decreased compared with the values obtained in the same group 2 rats during baseline conditions.

to the sclerotic glomeruli, but are also diffusely present in the nonsclerotic glomeruli (30). Furthermore, previous electron microscopic studies (6) in rats 1–2 wk after more extensive subtotal renal ablation demonstrated that the remnant glomeruli had an irregular detachment of podocytes and endothelial cells from the basement membrane. Large expanses of denuded basement membrane were present where the epithelial cells had become detached from the glomerular basement membrane.

It is conceivable, then, that the glomeruli after less severe NPX, such as those in our model, may have qualitatively similar, yet less extensive, changes of the glomerular capillary wall structure under the influence of ongoing high glomerular pressures. Such distortion of the capillary wall may represent the structural equivalent of the large pores and provide pathways more permeable to macromolecules. In these nephrons, the prevailing high glomerular pressure is an important determinant for the ongoing sieving defect. Finally, our observations raise the possibility that the reduction in proteinuria after

some therapeutic maneuvers (32, 33) may not reflect their structure-sparing effect on damaged glomeruli, which contribute little to the proteinuria. Instead, it may be attributed to their effect on intact glomeruli by reducing intracapillary pressure (34), to which protein transfer is highly sensitive.

Acknowledgments

The authors express their sincere gratitude to Dr. Helmut G. Rennke for his invaluable advice in preparing and analyzing radiolabeled dextrans. The authors wish to thank Mrs. Laurette Hughes and Mrs. Teresa Bills for technical assistance, and Ms. Mary E. Yeomans for secretarial work.

Dr. I. Ichikawa is a recipient of the Established Investigatorship Award from the American Heart Association. These studies were supported by the National Institutes of Health grants DK-37868 and DK-33501.

References

1. Myers, B. D., T. B. Okarma, S. Friedman, and C. R. Bridges. 1982. Mechanisms of proteinuria in human glomerulonephritis. *J. Clin. Invest.* 70:732–746.
2. Shemesh, O., J. C. Ross, W. M. Deen, G. W. Grant, and B. D. Myers. 1986. Nature of glomerular capillary injury in human membranous glomerulopathy. *J. Clin. Invest.* 77:868–877.
3. Shimamura, T., and A. B. Morrison. 1975. A progressive glomerulosclerosis occurring in partial five-sixths nephrectomized rats. *Am. J. Pathol.* 79:95–106.
4. Furkerson, M. L., P. E. Hoffsten, and S. Klahr. 1976. Pathogenesis of the glomerulopathy associated with renal infarction in rats. *Kidney Int.* 9:407–417.
5. Hostetter, T. H., J. L. Olson, H. G. Rennke, M. A. Venkatachalam, and B. M. Brenner. 1981. Hyperfiltration in remnant nephrons: a potentially adverse response to renal ablation. *Am. J. Physiol.* 241 (*Renal Fluid Electrolyte Physiol.* 10):F85–F93.
6. Olson, J. L., T. H. Hostetter, H. G. Rennke, and B. M. Brenner. 1982. Altered glomerular permselectivity and progressive sclerosis following extreme ablation of renal mass. *Kidney Int.* 22:112–126.
7. Ichikawa, I., D. A. Maddox, M. G. Cogan, and B. M. Brenner. 1978. Dynamics of glomerular ultrafiltration in euvoletic Munich-Wistar rats. *Renal Physiol.* 1:121–131.
8. Yoshida, Y., A. Fogo, A. D. Glick, and I. Ichikawa. 1988. Serial micropuncture analysis of single nephron function in chronic renal disease: a study in the rat model of subtotal renal ablation. *Kidney Int.* 33:855–867.
9. Deen, W. M., J. L. Troy, C. R. Robertson, and B. M. Brenner. 1973. Dynamics of glomerular ultrafiltration in the rat. IV. Determination of ultrafiltration coefficient. *J. Clin. Invest.* 52:1500–1508.
10. Ichikawa, I., J. M. Pfeffer, M. S. Pfeffer, T. H. Hostetter, and

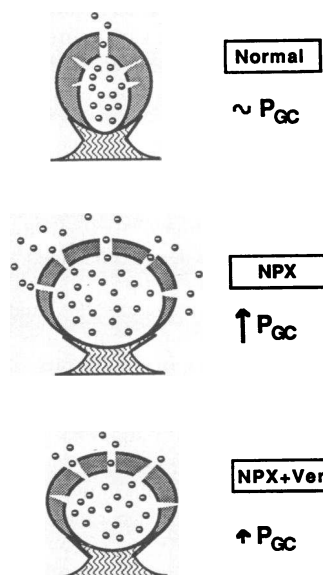


Figure 8. Dramatized scheme dictating the mathematical interpretation of the changes occurring in the channels for macromolecular transport in the glomerular capillary wall of remnant nephrons after subtotal NPX. Top, the normal condition of glomerular capillary membrane with normal glomerular capillary pressure (P_{GC}), in which small numbers of large nonselective pores are distributed among large numbers of small size-selective pores. In the baseline condition of remnant glomeruli (middle, NPX), an increase in large-to-small pore population ratio, which accounts for the observed increase in fractional volume flux through a nonselective pathway, is associated

with elevated P_{GC} . When the degree of high P_{GC} was lessened by verapamil infusion (shown on the bottom, NPX + Ver), the large-to-small pore population ratio decreased toward normal control level. The pore radii of small selective pores remained unaffected throughout the study.

B. M. Brenner. 1984. Role of angiotensin II in the altered renal function of congestive heart failure. *Circ. Res.* 55:669-675.

11. Weening, J. J., and H. G. Rennke. 1983. Glomerular permeability and polyanion in adriamycin nephrosis in the rat. *Kidney Int.* 24:152-159.

12. Yoshioka, T., T. Mitarai, V. Kon, W. M. Deen, H. G. Rennke, and I. Ichikawa. 1986. Role for angiotensin II in an overt functional proteinuria. *Kidney Int.* 30:538-545.

13. Yoshioka, T., H. G. Rennke, D. J. Salant, W. M. Deen, and I. Ichikawa. 1987. Role of abnormally high transmural pressure in the permselectivity defect of glomerular capillary wall: a study in early Passive Heymann Nephritis. *Circ. Res.* 61:531-538.

14. Führ, J., J. Kazmarczyk, and C. D. Krüttgen. 1955. Ein einfache colorimetrische Methode zur Inulinbestimmung für Nieren-clearanceuntersuchungen bei Stoffwechselfgesunden und Diabetikern. *Klin. Wochenschr.* 33:729-730.

15. Vurek, G. G., and S. E. Pegram. 1966. Fluorometric method for the determination of nanogram quantities of inulin. *Anal. Biochem.* 16:409-419.

16. Viets, J. W., W. M. Deen, J. L. Troy, and B. M. Brenner. 1978. Determination of serum protein concentration in nanoliter blood samples using fluorescamine or *O*-phthalaldehyde. *Anal. Biochem.* 88:513-521.

17. Bradford, M. M. 1976. A rapid and sensitive method for the quantitation of microgram quantities of protein utilizing the principle of protein-dye binding. *Anal. Biochem.* 72:248-254.

18. Voller, A., A. Bartlett, and D. E. Bidwell. 1978. Enzyme immunoassays with special reference to ELISA techniques. *J. Clin. Pathol.* 31:507-520.

19. Deen, W. M., C. R. Bridges, B. M. Brenner, and B. D. Myers. 1985. Heteroporous model of glomerular size-selectivity: application to normal and nephrotic humans. *Am. J. Physiol.* 249(Renal Fluid Electrolyte Physiol. 18):F374-F389.

20. Raij, L., S. Azar, and W. Keane. 1984. Mesangial immune injury, hypertension, and progressive glomerular damage in Dahl rats. *Kidney Int.* 26:137-143.

21. Wallenstein, S., C. L. Zucker, and J. Fleiss. 1980. Some statistical methods useful in circulation research. *Circ. Res.* 47:1-9.

22. Snedecor, G. W., and W. G. Cochran. 1967. Statistical Methods. 6th ed. The Iowa State University Press, Ames, IA. 135-171.

23. Fielding, B. A., D. A. Price, and C. A. Houlton. 1983. Enzyme immunoassay for urinary albumin. *Clin. Chem.* 29:355-357.

24. Mohamed, A., T. Wilkin, B. Leatherdale, and R. Davies. 1984. A microenzyme-linked immunosorbent assay for urinary albumin, and its comparison with radioimmunoassay. *J. Immunol. Methods.* 74:17-22.

25. Feldt-Rasmussen, B., B. Dinesen, and M. Deckert. 1985. Enzyme immunoassay: an improved determination of urinary albumin in diabetics with incipient nephropathy. *Scand. J. Clin. Lab. Invest.* 45:539-544.

26. Schwerer, B., M. Bach, and H. Bernheimer. 1987. ELISA for determination of albumin in the nanogram range: assay in cerebrospinal fluid and comparison with radial immunodiffusion. *Clin. Chem. Acta.* 163:237-244.

27. Oken, D. E., and W. Flamenbaum. 1971. Micropuncture studies of proximal tubule albumin concentrations in normal and nephrotic rats. *J. Clin. Invest.* 50:1498-1505.

28. Kincaid-Smith, P. 1973. The natural history and treatment of mesangiocapillary glomerulonephritis. In *Glomerulonephritis: Morphology, Natural History and Treatment*. Kincaid-Smith, P., T. H. Mathew, and E. L. Becker, editors. John Wiley & Sons, New York. 591-609.

29. Lavender, S., J. Bennett, P. F. Morse, and A. Polak. 1974. Albumin and creatinine clearances in renal disease. *Clin. Sci. Mol. Med.* 45:775-784.

30. Goldszer, R. C., J. Weet, and R. S. Cotran. 1984. Focal segmental glomerulonephritis. *Annu. Rev. Med.* 35:429-450.

31. Shemesh, O., W. M. Deen, B. M. Brenner, E. McNeely, and B. D. Myers. 1986. Effect of colloid volume expansion on glomerular barrier size-selectivity in humans. *Kidney Int.* 29:916-923.

32. Anderson, S., T. W. Meyer, H. G. Rennke, and B. M. Brenner. 1985. Control of glomerular hypertension limits glomerular injury in rats with reduced renal mass. *J. Clin. Invest.* 76:612-619.

33. Nath, K. A., S. M. Kren, and T. H. Hostetter. 1986. Dietary protein restriction in established renal injury in the rat. Selective role of glomerular capillary pressure in progressive glomerular dysfunction. *J. Clin. Invest.* 78:1199-1205.

34. Heeg, J. E., P. E. de Jong, G. K. van der Hem, and D. de Zeeuw. 1987. Reduction of proteinuria by angiotensin converting enzyme inhibition. *Kidney Int.* 32:78-83.